ELSEVIER

Applied Surface Science 113/114 (1997) 680–684

applied
surface science

Single-layer halftone phase-shifting masks for DUV microlithography: optical property simulation and chromium compound film preparation

Zhong-Tao Jiang [a,*], Seungbum Hong [a], Eunah Kim [a], Byeong-Soo Bae [a], Sungchul Lim [b], Sang-Gyun Woo [b], Young-Bum Koh [b], Kwangsoo No [a]

[a] *Department of Materials Science and Engineering, Korea Advanced Institute of Science and Technology, Taejon, South Korea*
[b] *Samsung Electronics Co., Ltd., Yongin-gun, Kyongki-do, South Korea*

Abstract

The investigation of single layer halftone phase shift mask (SLHTPSM) has been carried by both simulation and chromium fluoride film fabrication. Theoretical analysis provides the optimum SLHTPSM constructions for I-line (365 nm), KrF (248 nm) and ArF (193 nm) microlithographies. A fully characterization of chromium fluoride film processed by dc magnetron sputtering shows a feasibility of using this film in the fabricating DUV-PSM.

PACS: 85.40.Hp

Keywords: DUV-lithography; Simulation; Phase-shifting mask; CrF film; Dc sputtering

1. Introduction

Recently microlithography technology is going to the pattern dimensions of less than 200 nm. Except X-ray and E-beam, it is possible that using deep-UV optical projection lithography combined with resolution enhanced technologies, such as phase shift mask (PSM), off-axis illumination and pupil filter to fabricate 1 Gbit (or 4 Gbit) DRAM with the minimum feature size in the region of 200 to 150 nm. The halftone phase-shifting mask is one of the most practical technologies to enhance the pattern resolution which consists of a transparent substrate and an attenuated halftone layer with a limited optical transmittance up to 20%. The attenuated layer also makes 180° phase-shifting with respect to the apertures playing a role in reducing the size of bright feature on the wafer (see Fig. 1a). By using this technology, the mask design with intermediate transmittance values is effective for fabricating isolated hole patterns because it does not require a special layout design [1,2]. Since 1993, single-layer halftone phase-shifting mask (SLHTPSM) has been investigated and developed extensively [3–6], where the single layer film controls both transmittance and phase-shifting. Proper combinations of refractive index (n) and extinction coefficient (k) can be achieved to deliver the needed transmittance (T) and phase-shifting (φ) at reasonable film thickness (d) by changing the mixing ratio of two (or three) selected materials and

* Corresponding author.

0169-4332/97/$17.00 Copyright © 1997 Elsevier Science B.V. All rights reserved.
PII S0169-4332(96)00933-6

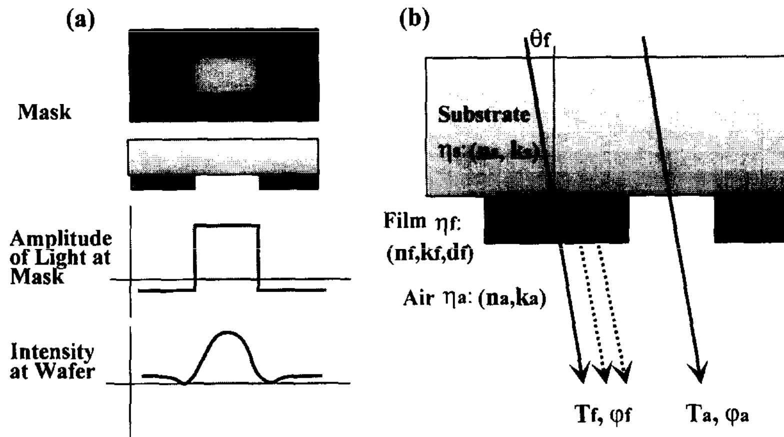

Fig. 1. Halftone phase-shifting mask: (a) structure and transmitted light intensity; and (b) physical model of non-multi reflection effect (solid light lines) and multi reflection effect (solid + dotted light lines) in SLHTPSM.

deposition parameters. In this circumstance, the system simulation is extremely important and helpful to find some suitable combinations of these optical properties.

In the present paper, we will study the optimum construction of SLHTPSM for 248 nm and 193 nm optical-lithography. Real mask film investigation will be focused on the characterization of chromium fluoride processed by dc magnetron sputtering interpenetration with simulation predictions.

2. Optical simulation

A physical model for SLHTPSM can be designed as shown in Fig. 1b with the basic requirements to be: (i) $T'_{PSM} = T_f/T_a = 5\%$ (or up to 20%); and (ii) $\varphi'_{PSM} = \varphi_f - \varphi_a = 180°$. The optical parameters: (n_s, k_s), (n_f, k_f), and (n_a, k_a), are for the substrate, single layer phase-shifting film and air, respectively. d_f is the thickness of the single layer phase-shifting film. The substrate is considered as a semi-infinite media. Full derivation of optical simulation has been given in Ref. [7] which includes a prime study of non-multi reflection analysis and matrix approach. Starting from non-multi reflection model which provides the initial values of k_f and d_f for a certain refractive index (n_f), the simulation process calculates the T_{PSM} and φ_{PSM}. By changing the d_f and k_f values, the transmittance difference ($T'_{PSM} - T_{PSM}$) and phase-shifting difference ($\varphi'_{PSM} - \varphi_{PSM}$) are approached to near zero. Then the optimized combination of n_f, k_f, and d_f of a given system are achieved.

Simulation process described above has be verified by the optical characterization data of the thermal oxidation processed single-layer chrome mask film on Quartz substrate [4] and $(LaNiO_3)_x(Ta_2O_5)_{1-x}$ oxide thin films. Good correlations have been obtained between the experimental and theoretical results [7].

3. Experimental

Chromium fluoride films were deposited using planar circular type dc magnetron reactive sputtering system with a ring-shaped 4″ Cr target. The Cr target (99.95% purity, Cerac, Inc.) was 1/4″ thick and mechanically clamped to a water-cooled copper electrode. The target to substrate distance and gas ring were fixed to be 132.4 and 30 mm, respectively. A mesh was inserted below gas ring in order to increase the film uniformity. The Ar + CF_4 gas outlet in the gas ring was directed 45° downward. The deposition conditions are dc power of 109 W and chamber working pressure of about 5 mTorr at room temperature. Films were deposited on slide glass, quartz and Si substrates simultaneously. The CF_4 gas flow was varied from 0.6 to 1.0 sccm while the total reaction gas (Ar + CF_4) flow rate was fixed as 10

sccm. The film characterizations were carried out by XRD, α-step and spectroscopic ellipsometer (SOPRA SE ESVG).

4. Results and discussion

4.1. The optimized SLHTPSM structure for DUV-lithographs

A theoretical analysis based on the simulation process shows that, in the case of a given λ and d_f, the changing of the k_f value strongly affects the transmittance but only weakly affects the phase-shifting while n_f value remains constant. However, the changing of the n_f value, while keeping the k_f value constant, causes a relatively small change for transmittance but a large change for phase shifting.

The optimized SLHTPSM film structure for DUV-lithography application can be derived without much difficulty by using this simulation process. Fig. 2 shows the relationship among the optimized k_f, n_f and d_f values to be matched the requirements of SLTHPSM for 365, 248 and 193 nm exposure lights. The optimum tolerance is less than 2% and 0.5% for transmittance and phase-shifting, respectively. Three curves of optimized k_f corresponding to the 365 nm, 248 nm and 193 nm wavelengths for each transmittances nearly overlap together clearly indicates that, over a wide wavelength range, the optimized k_f is only very weakly effected by the exposure wavelength (λ). Simulation process also reveals that at refractive index (n_f) values < 2.5 transmittance variations in the range 5–20% have no effect on optimized mask thickness (d_f) and at values above this, between 2.5 and 6, that there is slight dispersion which is just a broadening of the line. A further analysis indicates that 1% of margin tolerance for the d_f will create about 2.5% difference for transmittance and about 1% difference for phase-shifting under the given λ, n_f and k_f values. The film transmittance, in the case of SLHTPSM, can be mainly adjusted by k_f because the d_f is restricted by the 180° phase-shifting requirement. Simulation process also indicates, within a wide exposure wavelength region, the margin tolerance of d_f makes a similar effect on the transmittance and phase-shifting over the considerable n_f range. The higher n_f value, however, needs a smaller d_f to match the target requirements, and it would cause more difficulties in controlling the accuracy of the d_f during the fabrication, so that the high refractive index film materials (e.g., $n_f > 3$) are not the feasible candidates for

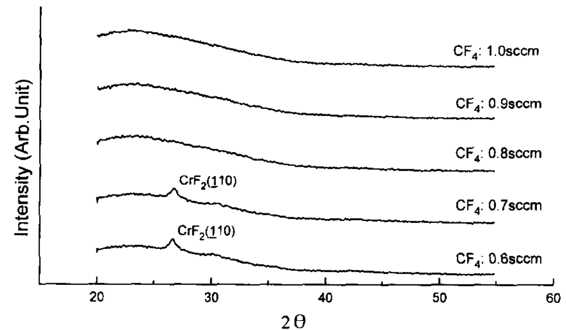

Fig. 3. XRD patterns of the CrF film for the various deposition CF_4 flow rates.

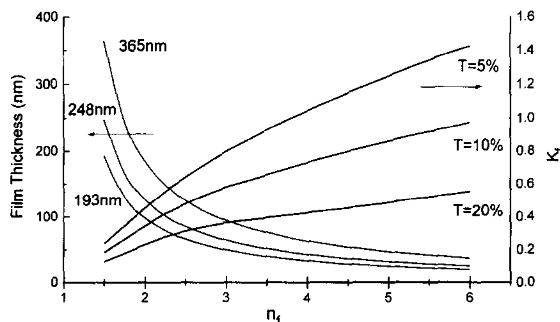

Fig. 2. The optimized combinations of k_f, d_f and n_f for the transmittance of 5%, 10% and 20%, and the phase shift of 180(±0.5%)° at 365, 248 and 193 nm, where n_s is 1.507.

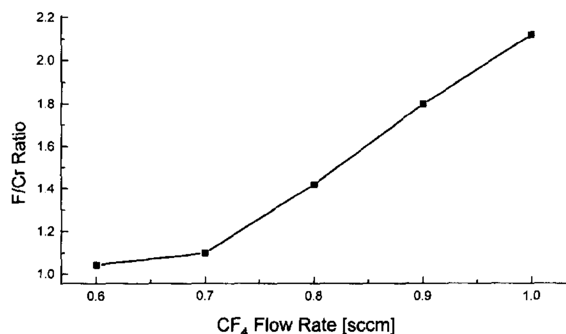

Fig. 4. Film F/Cr composition ratio as function of CF_4 flow rate on Si substrate.

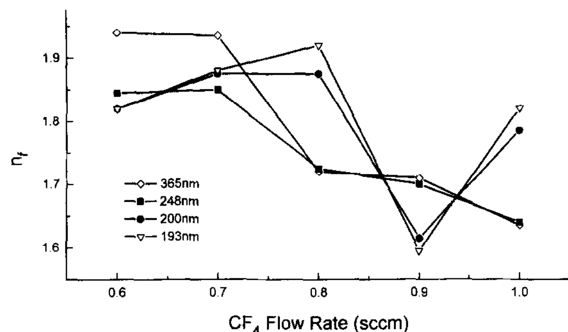

Fig. 5. CF_4 flow rate dependence of n_f at 365, 248 and 193 nm wavelengths.

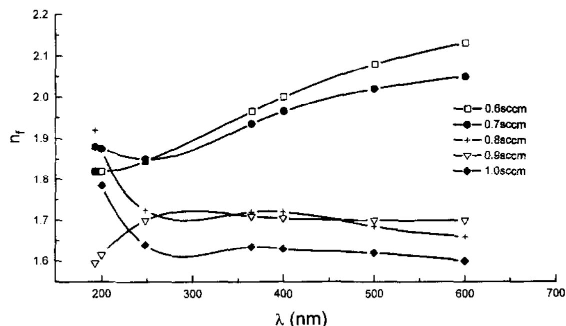

Fig. 7. Refractive index (n_f) of CrF film for the different CF_4 flow rates.

SLHTPSM in the DUV lithography especially for the 193 nm exposure wavelength application.

4.2. Chromium fluoride film characterization

The effects of the reaction gas flow rate ratio, $CF_4/(Ar + CF_4)$, and the deposition parameters on the film phase transformation, composition and optical properties were evaluated. XRD analysis indicated the film phase transformed from polycrystalline to amorphous while the CF_4 flow rate increased from 0.6 to 1.0 sccm (Fig. 3). Fig. 4 shows that the F/Cr composition ratio increases as the CF_4 flow rate increases. The optical transmittance of CrF film increasing while the film turning from polycrystalline to amorphous phase is due to the less effect of light-scattering by grain-boundaries in the film. Figs. 5–8 are the plots of the dependence of n_f and k_f values on CF_4 flow rate and wavelength, respectively. It indicts that the n_f and k_f values could be adjusted in quite large ranges (e.g., 1.6–1.95 for n_f and 0.1–0.6 for k_f) by varying the CF_4 flow rate, while remaining the other deposition parameters as constant, for fitting the different exposure wavelengths in the application of Att-mask. By employing the simulation program, suitable CrF film thicknesses for different exposure wavelengths have be found. The calculated wavelength dependent transmittance based on the known n_f and k_f values have good agreement with the corespondent experiment results. In order to study the absorption edge for all the cases, the calculated transmittance, film thickness to be converted to 150 nm, are displayed in Fig. 9. The CrF film absorption edge shifts to shorter wavelength as increasing of the CF_4 flow rate (or F/Cr composition ratio) means the band gap becomes wider. It could be explained as Mott gap excitation [8] which is formed between the F 2p valence band and the Cr 3d conduction band. The weaker optical transition in the higher photon energy is consistent

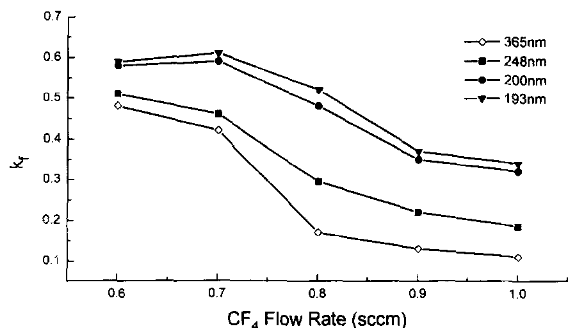

Fig. 6. CF_4 flow rate dependence of k_f for 365, 248 and 193 nm wavelengths.

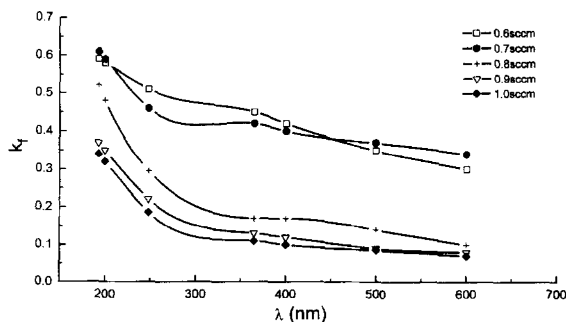

Fig. 8. Extinction coefficient (k_f) of CrF film for the different CF_4 flow rates.

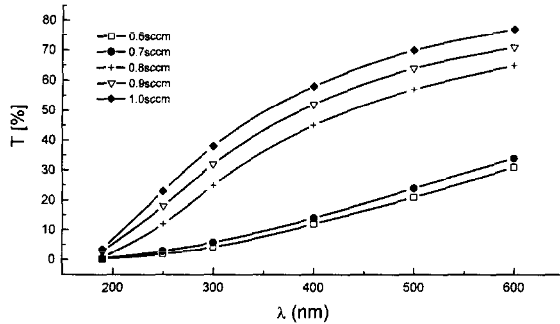

Fig. 9. Transmittance of CrF film for the various deposition CF_4 flow rates ($d_f = 150$ nm).

with the general tendency that the electron correlation becomes stronger as the F/Cr atomic ratio approaches to one.

5. Conclusions

A physical model and simulation program for SLHTPSM established and verified previously derives the optimized combination of k_f/n_f and d_f/n_f of SLHTPSM to achieved the 5%, 10% and 20% transmittance and 180° phase-shifting for 365, 248 and 193 nm microlithographies, as well as provides evidence that the reasonable refractive index value for the SLHTPSM might be in the region of 1.7–3. Theoretical analyses indicate that, for the given λ and d_f, the transmittance and phase-shifting are mainly controlled by k_f and n_f and weakly affected by n_f and k_f of the attenuated film, respectively. Higher refractive index mask materials cause more difficulties in fabricating a good quality phase-shifting masks. The characterization of CrF films shows that the film n, k and T values, and absorption edge can be controlled by varying the CF_4 flow rate during the deposition process to satisfy the requirements of SLHTPSM in the application of DUV-lithography.

References

[1] M.D. Levenson, N.S. Viswanathan and R.A. Simpson, IEEE Trans. Electron Devices ED-29(12) (1982) 1828.

[2] T. Terasawa, N. Hasegawa, H. Fukuda and S. Katagiri, Jpn. J. Appl. Phys. 30(11B) (1991) 2991.

[3] M. Nakajima, N. Yoshioka, J. Miyazaki, H. Kusunose, K. Hosono, H. Morimoto, W. Wakamiya, K. Murayama, Y. Watakabe and K. Tsukamoto, Proc. SPIE 2197 (1994) 111.

[4] D.S. O'Grady and P.B. Wilber, Proc. SPIE 2197 (1994) 194.

[5] K. Kawano, M. Asano, S. Tanaka, T. Iwamatsu, H. Sato and S. Ito, Proc. SPIE 2512 (1995) 348.

[6] S.I. Ito, H. Hazama, T. Kamo, H. Miyazaki, H. Sato, K. Hayashi, H. Shigemitsu and I. Mori, Proc. SPIE 2197 (1994) 99.

[7] Z.-T. Jiang, S. Hong, E. Kim, B.-S. Bae, K. No, S.-C. Lim, S.-G. Woo and Y.-B. Koh, Semiconductor Sci. Technol. 11(10) (1996) 1450.

[8] T. Arima, Y. Tokura and J.B. Torrance, Phys. Rev. B 48 (1993) 17006.